Science of the Total Environment 663 (2019) 144–153

Contents lists available at ScienceDirect

Science of the Total Environment

journal homepage: www.elsevier.com/locate/scitotenv

A hybrid modeling framework to estimate pollutant concentrations and exposures in near road environments

Fatema Parvez, Kristina Wagstrom *

Department of Chemical and Biomolecular Engineering, University of Connecticut 191 Auditorium Road, Unit 3222. Storrs, CT 06269-3222, United States of America

HIGHLIGHTS

- Assessing exposure requires detailed spatiotemporal air pollutant concentrations.
- This approach estimates hourly air pollutant concentrations at 40 m × 40 m resolution.
- Air pollutant concentrations vary significantly by hour of the day and the season.
- 40 m × 40 m estimates lead to higher average exposure concentrations than 12 km × 12 km.
- This model, HYCAMR, efficiently provides needed estimates for exposure assessment.

GRAPHICAL ABSTRACT

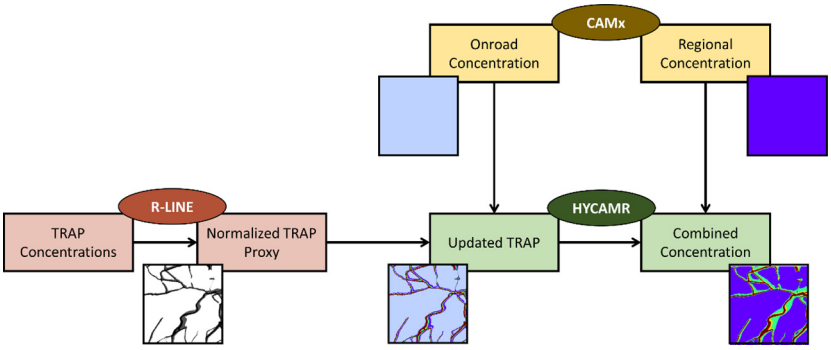

ARTICLE INFO

Article history:
Received 5 October 2018
Received in revised form 3 January 2019
Accepted 18 January 2019
Available online 19 January 2019

Editor: Pavlos Kassomenos

Keywords:
Air pollution
Traffic-related air pollution
Near road concentrations
Air pollution modeling
Exposure assessment

ABSTRACT

Traffic related air pollution is one of the major local sources of pollution challenging most urban populations. Current air quality modeling approaches can estimate the concentrations of air pollutants on either regional or local scales but cannot effectively estimate concentrations from the combination of regional and local sources at both local and regional scales simultaneously. This study describes a hybrid modeling framework, HYCAMR, combining a regional model, CAMx, and a local-scale dispersion model, R-LINE, to estimate concentrations of both primary and secondary species at high temporal (hourly) and spatial (40 m) resolution. HYCAMR utilizes all the chemical and physical processes available in CAMx and the Particulate Matter Source Apportionment Technology (PSAT) tool to estimate concentrations from both onroad and nonroad emission sources. HYCAMR employs R-LINE, to estimate the normalized dispersion of pollutant mass from onroad emission sources, from primary and secondary roads, at high resolution. Applying R-LINE for one day per month using average daily meteorology yields seasonally-resolved spatial dispersion profiles at low computational cost. Combining the R-LINE spatial dispersion profile with CAMx concentration estimates yields an estimate of the combined concentrations for a range of pollutants at high spatial and temporal resolution. In three major cities in Connecticut, HYCAMR shows strong temporal and seasonal variability in NOx, $PM_{2.5}$, and elemental carbon (EC) concentrations. This study evaluates HYCAMR year 2011 estimates of NO_2 and $PM_{2.5}$ against two sources: satellite-based estimates at coarse resolution and regression model estimates at census block group resolution. In this evaluation, HYCAMR demonstrates improved agreement with the land-use regression modeling and mixed agreement with satellite-based estimates when compared to the regional CAMx estimates.

* Corresponding author at: Chemical & Biomolecular Engineering, 191 Auditorium Road, Unit 3222, Storrs, CT 06269-3222, United States of America.
E-mail addresses: fatema.parvez@uconn.edu (F. Parvez), kristina.wagstrom@uconn.edu (K. Wagstrom).

https://doi.org/10.1016/j.scitotenv.2019.01.218
0048-9697/

1. Introduction

Motor vehicles are one of the most significant anthropogenic sources of air pollution in urban areas. In addition, the rapid growth of the world's motor-vehicle fleet resulting from population growth, economic growth, metropolitan expansion, and increased dependence on motor vehicles has resulted in an increase in the number of people living and working near major roads (Adar and Kaufman, 2007; Salam et al., 2008). Negative health outcomes associated with traffic-related air pollution include asthma (Vette et al., 2013; Jerrett et al., 2008; Rohr et al., 2014), respiratory impacts (Kim et al., 2015; Winquist et al., 2015; Pascal et al., 2014), cardiovascular impacts (Franck et al., 2011; Crouse et al., 2012), cancer (Arden Pope et al., 2011; Turner et al., 2011; Loomis et al., 2013), low birth weight (Wilhelm et al., 2012; Bell et al., 2008; Ebisu and Bell, 2012), and premature death (Schwartz et al., 2008; Pope et al., 2009; Crouse et al., 2012). A special report on traffic related air pollution by the Health Effects Institute (HEI, 2010) identified a heightened exposure zone within a range extending to somewhere between 300 m and 500 m from major roads. Much of the area in this zone may experience concentrations 2.5 to 6 times higher than the background. There is an urgent need to estimate near road pollutant concentrations at high resolution to improve exposure estimates.

Scientists and policy makers typically estimate ambient air pollutant concentrations using either data from air quality monitoring networks or from air pollution models. Both of these methods have limitations. A major limitation associated with monitored concentrations is the relatively low spatial resolution and spatial coverage associated with most networks. It is also challenging to estimate source specific contributions to air pollutant concentrations using monitored values. Caiazzo et al. (2013) estimated that, in 2005, road sources accounted for 38.5% of total NO_x and 6.9% of total $PM_{2.5}$ emissions in the United States. Dedoussi and Barrett (2014) attributed 7826, 3982, and 3702 premature death in 2005 in California, New York, and New Jersey, respectively, due to exposure to traffic-related pollution. Unfortunately, current regulatory ambient air monitoring does not adequately capture near road concentration levels for most locations and chemical species. For this reason, regulators need high spatial and temporal resolution modeling approaches to accurately estimate exposure for a wide variety of chemical species.

The air quality modeling approaches currently available can compute the source-specific pollutant concentrations either on a regional- or local-scale but still lack effective ways to estimate the combined exposure from regional and local sources. Fann et al. (2013) used the CAMx regional air pollution model (12kmx12km resolution) to quantify ozone and $PM_{2.5}$ related premature deaths from onroad emission sources in the United States. As elevated concentrations near roads reach background levels within a few hundred meters, regional air pollution models which can, at most, resolve down to 1 km cannot adequately represent these gradients. Further, temporal variabilities in pollutant dispersion patterns in stable and unstable atmospheric conditions also greatly influence the concentration gradients near roads. Estimating air pollution from local sources such as motor vehicles using a regional air pollution model which considers all the processes that impact atmospheric chemistry and physics is a computationally intensive process. A potentially better, and more realistic approach, is to use local scale dispersion models for near road air pollution estimation. Compared to chemical transport model (CTMs), local scale dispersion models are less computationally expensive and can provide concentration estimates at high resolution. Batterman et al. (2015) implemented the R-LINE, a local scale dispersion model, to quantify spatially resolved $PM_{2.5}$ and NOx concentrations in Detroit, MI. Greco et al. (2007) estimated traffic related exposures using a line source model, CAL3QHCR, in Boston, MA. Traditionally, the dispersion models available to estimate near road pollutant concentrations either do not account for background concentrations from regional sources, do not account for temporal variability, or do not consider chemical interactions between local and regional pollutants. There remains a need to better quantify the combined local and regional pollution impact to design effective policies to protect human health from the harmful effects of air pollution exposure.

Researchers have recently started to develop hybrid models to bridge this gap between local and regional air pollution modeling. Isakov et al. (2007) combined a regional and dispersion model to evaluate the sub-grid temporally- and spatially-resolved benzene and formaldehyde concentrations from vehicular emissions. Beevers et al. (2012) also applied a similar modeling approach to estimate NOx and ozone concentrations at 20mx20m resolution. Both of these approaches provide fine temporal and spatial scale concentration estimates that can aid in health impact assessments and epidemiological studies. However, these approaches potentially lead to over-estimation of pollutant concentrations due to the double counting emissions by considering the same emissions in both models. Bates et al. (2018) developed a hybrid modeling framework combining CMAQ and R-LINE to quantify pollutants concentrations at a neighborhood scale. Chang et al. (2015) employed a hybrid approach in central North Carolina and estimated near road $PM_{2.5}$ concentrations at a Census block resolution. Both these approaches provide better concentration characterization in terms of spatial resolution but lack temporal resolution. Running the model multiple times for multiple species makes these modeling approaches also data intensive. Most of the hybrid modeling frameworks currently available either double count onroad emissions, do not provide temporal information, need extensive additional data, or require significant computational resources due to the required number of model runs.

Here we present a hybrid modeling framework (HYCAMR) combining a regional chemical transport model and a local scale road dispersion model to estimate combined (regional and local/near road) concentrations at fine spatial and temporal resolution. We employ HYCAMR in three Connecticut cities - Hartford, New Haven, and Willimantic - to estimate hourly $PM_{2.5}$, NOx, and elemental carbon (EC) concentrations at a 40mx40m resolution. This approach provides improved spatial and temporal resolution of concentrations profiles in near road environments to improve exposure assessment.

2. Method and model description

Our hybrid modeling framework, HYCAMR, is comprised of an Eulerian 3-D chemical transport model, the Comprehensive Air Quality Model with Extensions (CAMx version 6.0), and a local scale road dispersion model, R-LINE-v1.2. Fig. 1 shows a diagram of the information flow within HYCAMR. HYCAMR uses CAMx to define the regional contributions and also to determine the mass of pollutant originating from local, onroad emissions. HYCAMR uses R-LINE to determine the dispersion pattern of the local, onroad emissions. By combining the results from both models, HYCAMR provides an estimate of the total pollutant concentration for each hour of the year at 40mx40m resolution. We describe the details of HYCAMR in Sections 2.1–2.3.

2.1. Regional-scale estimates (CAMx)

In HYCAMR, we use the Comprehensive Air Quality Model with Extensions (CAMx) to quantify the concentrations of various species from onroad and regional sources in the Northeastern US with a grid resolution of 12kmx12km. We apply the Lambert Conformal Projection over the studied domain with 6834 ground-level grid cells (67 north-south x 102 east-west) and 20 vertical layers. CAMx uses first principles to estimate the impacts of emissions, advection, turbulent diffusion, condensation, evaporation, deposition, and chemical reactions (gaseous and aqueous) on air pollutant concentrations. We implement the Particulate Matter Source Apportionment Technology (PSAT) tool available in CAMx to separately track the transport and transformations of species from onroad and regional emission sources. We use the 2011 National Emissions Inventory (NEI) developed by the US Environmental Protection Agency (EPA) processed using the Sparse Matrix Operator Kernel

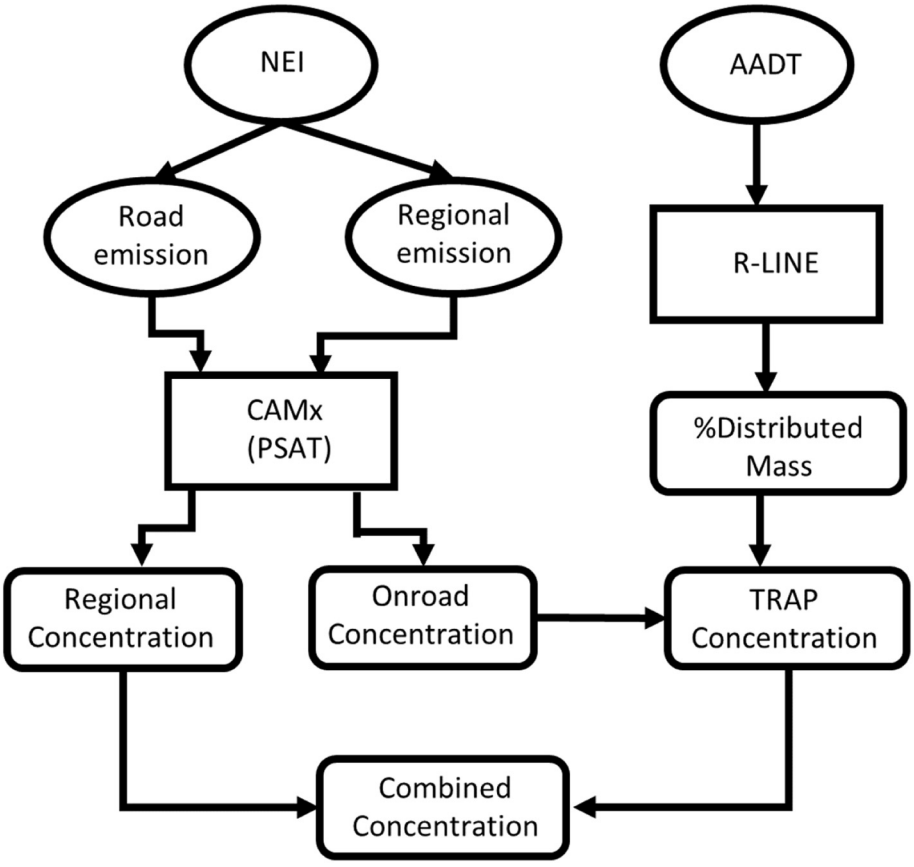

Fig. 1. Schematic of our hybrid modeling framework, HYCAMR. NEI and AADT denote the National Emission Inventory and Annual Average Daily Traffic dataset, respectively.

Emissions (SMOKE) (CMAS, 2013) model. These emissions inputs were included as part of the United States Environmental Protection Agency's Ozone Regulatory Reanalysis, including model evaluation (US EPA, 2014a). For gas phase chemistry, we use CAMx mechanism 7. This mechanism is based on the Carbon Bond version 6 (CB-6) (Yarwood et al., 2010) mechanism and includes aerosol chemistry. CAMx mechanism 7 has a total of 218 reactions for 77 gaseous species and includes 16 aerosol species. In CAMx, $PM_{2.5}$ includes secondary nitrate, sulfate, ammonium, organic aerosols, and several primary species. We create boundary conditions for the New England domain using a CAMx run for the continental US using the same inputs. We use meteorological inputs predicted by the Weather Research and Forecasting model WRF (version 3.4) (Skamarock et al., 2008). The WRF domain includes 471 × 311 cells with a horizontal resolution of 12kmx12km over the United States. The vertical grid has 35 sigma levels stretching from near surface to 50 hPa. The meteorological model evaluation is provided in US EPA's Meteorological Model Performance report 2011 (US EPA, 2014b). Parvez et al. (2017) contains a detailed performance evaluation of CAMx estimates using this set of inputs.

Using these datasets, we create two emission categories - onroad and all other sources. More specifically, we track the onroad emissions from each grid cell in each city as a separate source for use in HYCAMR (described in Section 2.3). We use these separated emissions in PSAT to track concentrations from onroad and other sources individually. We use this approach later to avoid double counting emissions. In the combined model, CAMx not only accounts for the chemistry of regional pollutants but also local onroad pollutants throughout PSAT.

2.2. Local-scale estimates (R-LINE)

R-LINE is a steady state Gaussian plume line source dispersion model developed by US EPA to estimate pollutant concentrations near roads. This model numerically integrates over multiple point sources to approximate emissions occurring along a line (Snyder et al., 2013). R-LINE includes both vertical and lateral dispersion, simulates low wind meander conditions, and applies Monin-Obukhov similarity theory for vertically profiling the wind and turbulence near the surface. For simplicity in this initial implementation of HYCAMR, we consider only primary and secondary roads.

Like other dispersion models, R-LINE typically uses meteorology from a nearby weather station. For consistency between CAMx and R-LINE, we use the same WRF-predicted meteorology for both R-LINE and CAMx (described in Section 2.1). We have compared this approach with using nearby weather station data in past work (Parvez and Wagstrom, 2018). We use the Mesoscale Model Interface Program (MMIFv3.2-beta) (EPA, 2015) to process meteorology and surface characteristics variables from WRF for use by R-LINE. MMIF considers the height of the lowest sigma level mid-point (~10 m) in computing meteorology inputs for dispersion models. The MMIF processed meteorological file contains 18 parameters representing near surface characteristics including friction velocity, wind speed, boundary layer depth, temperature, and convective velocity scale. Instead of using meteorology specific to each hour of the year, we consider daily hourly-resolved meteorology averaged over each month of the year 2011. For example, instead of model 1:00 am on each day of October, we average the meteorological conditions present at 1:00 am each day of October and run R-LINE for these average conditions. This provides 288 meteorological proxies representing one diurnal profile for each month.

In HYCAMR, R-LINE (version 1.2) provides spatially- and temporally-resolved near road pollutant dispersion profiles at high resolution. To do this, we run R-LINE using each of the 288 meteorological proxies described above to estimate spatial pollutant concentrations. This provides an estimate of pollutant spatial distribution representing a typical hour of the day of each month. We implement R-LINE in each

individual CAMx grid cell within each city of interest with a receptor spacing of 40 m yielding an estimate of near road pollutant concentrations at 40mx40m resolution. We use these estimated concentrations to create spatial proxies over which we distribute the hourly onroad source mass predicted by CAMx-PSAT. We describe this step in more detail in Section 2.3. This transforms the 288 proxies into hourly concentrations throughout the year (covering 8760 h) without needing to run R-LINE for every single hour of the year. This decreases the R-LINE computational burden by over an order of magnitude.

We use the Annual Average Daily Traffic (AADT) data from Connecticut Department of Transportation (CT DOT, 2011) for vehicle counts on major roads in the cities of interest. As mentioned earlier, we use R-LINE to quantify the relative dispersion of mass rather than the absolute concentrations. Applying an assumption of negligible chemistry and deposition, each species should follow the same anticipated dispersion pattern no matter the emissions rate. This allows us to use a simplified emission factor of 1 g/(ms) for each vehicle per day on each road. We designed this approach to minimize the computational burden associated with needing separate model runs for each species. For road location, we use the primary and secondary roads defined in the TIGER/Line shapefiles developed by the United States Department of Agriculture and available through the Geospatial Data Gateway (USDA, 2015). We have included maps of the roads in the Supporting information (Fig. S1).

2.3. Hybrid model (HYCAMR)

In the HYCAMR, we combine the CAMx estimated regional concentrations with R-LINE-estimated local dispersion to estimate total hourly pollutant concentrations at 40mx40m resolution. Using the R-LINE-predicted concentrations described in Section 2.2, we create the predicted pollutant dispersion pattern by normalizing each by the mass at each 40 m spaced receptor by the total mass within the CAMx grid cell (Eq. (1)).

$$f_i = \frac{R_i}{\sum_1^n R_i} \tag{1}$$

In Eq. (1), f_i is the fractional contribution at receptor location i, R_i is the R-LINE-predicted near road pollutant concentrations at receptor location i and n is the total number of receptor locations. We then distribute the CAMx-predicted onroad source concentration over the R-LINE-predicted normalized dispersion profile (f_i) to estimate near road pollutant concentrations at high resolution (Eq. (2)).

$$C_{L,i} = C_{L,CAMx} \times f_i \times \frac{V_{12km}}{V_{40m}} \tag{2}$$

In Eq. (2), $C_{L,i}$ is the near road pollutant concentrations at receptor location i, $C_{L,CAMx}$ is the CAMx-predicted onroad source concentration, and V_{12km} and V_{40m} are the resolution of the CAMx and R-LINE models, respectively. Once we estimate the concentrations from onroad sources at high resolution, we can simply add the regional concentration to estimate the total pollutant concentration at high resolution (Eq. (3)).

$$C_{Comb,i} = C_{L,i} + C_{R,CAMx} \tag{3}$$

In Eq. (3), $C_{Comb,i}$ is the combined regional and local pollutant concentrations at receptor location i and $C_{R,CAMx}$ is the CAMx-predicted regional concentration. We include a simplified, example calculation in the Supporting information (Section S2).

2.4. Model evaluation approach

Traditionally, developers evaluate the performance of air quality models using measurements. Due to the lack of availability of measurements in our domain at such a fine scale resolution, we instead evaluate the performance of HYCAMR with two other approaches to estimate fine scale concentrations: one based on land-use regression modeling (at census block group resolution) and one based on downscaled satellite measurements (at 0.01° × 0.01° resolution).

We evaluate HYCAMR performance for NO_2 and $PM_{2.5}$ in the year 2011 using two datasets: satellite-based estimates and land use regression estimates. We estimate satellite-based ground level NO_2 mixing ratio at Ozone Monitoring Instrument (OMI) resolution (0.05° × 0.05°) using an approach similar to the one described in Lamsal et al. (2008) (Eq. (4)). This approach uses a chemical transport model (GEOS-Chem) to estimate ground-level concentrations from satellite-measure NO_2 column density.

$$S_o = \frac{\nu S_G}{\nu \Omega_G - (\nu - 1)\Omega_G^F} \times \Omega_o \tag{4}$$

In Eq. (4), S represents the surface-level NO_2 mixing ratio and Ω represents the tropospheric NO_2 column density. The subscripts "O" and "G" represent OMI and GEOS-Chem, respectively. The OMI-derived surface NO_2 (S_O) represents the mixing ratio at the lowest vertical grid. ν represents the ratio of the local OMI NO_2 column to the mean NO_2 across the GEOS-Chem domain (2° × 2.5° resolution). Ω_G^F is the free tropospheric NO_2 column over the GEOS-Chem grid cell. The GEOS-Chem development team routinely compares model performance to a set of standard benchmarks (GEOS-Chem v9-02 benchmark history, 2017). For satellite data, we use the Berkeley High-Resolution (BEHR v3.0A) processed OMI NO_2 column density (Laughner et al., 2016) for our analysis. Finally, we compare this estimate of ground-level NO_2 with both HYCAMR and CAMx estimated concentrations. We also compare the HYCAMR and CAMx estimated NO_2 concentrations with Kim land use regression (Kim LUR) model estimates at census block group resolution developed by Kim et al. (2018). They employed a modeling approach to estimate the concentrations of the six criteria pollutants within each census block group in the contiguous United States for the years 1979–2015. Their modeling approach uses a universal kriging framework that includes summary predictors, estimated by partial least squares (PLS) from geographical variables, and spatial correlation..

To evaluate performance for $PM_{2.5}$, we compare the HYCAMR and CAMx estimated concentrations with combined geophysical-statistical model estimated concentrations with a resolution of 0.01° × 0.01°. This model estimates ground-level $PM_{2.5}$ by combining Aerosol Optical Depth (AOD) retrievals from the NASA Moderate Resolution Imaging Spectroradiometer (MODIS), Multi-angle Imaging Spectroradiometer (MISR), and Sea-Viewing Wide Field-of-View Sensor (SeaWIFS) instruments with the GEOS-Chem. GEOS-Chem is further calibrated to global-based observations using a geographically-weighted regression (GWR) (Van Donkelaar et al., 2016). The estimated $PM_{2.5}$ concentrations using GWR were highly consistent ($R^2 = 0.81$) with out-of-sample cross-validated $PM_{2.5}$ concentrations from monitors. We also again compare the estimates to the Kim LUR-estimated $PM_{2.5}$ concentrations. We include the definitions of each statistical quantity used in the model evaluation in the Supporting information.

3. Results

3.1. Seasonal variation of pollutant concentrations

We estimate the seasonal average concentration fields for NOx (NO, NO_2, N_2O_5, radical NO_3, and HONO), $PM_{2.5}$, and elemental carbon (EC) using HYCAMR in New Haven, Hartford, and Willimantic (Figs. 2 and S3–S4). We see substantial seasonal variation in the dispersion pattern between species and locations. The differences in the spatial dispersion between seasons mostly results from meteorological differences though we do account for changes in emissions at both regional and local scales through the use of CAMx concentrations for both sets of sources,

regional and onroad (Section 2.3). We see the highest concentrations in winter due to the lower mixing heights, friction velocities, and convective velocities that hinder the dispersion of pollutants. Conversely, high wind speeds in spring facilitate rapid dispersion leading to lower concentrations near the road and decreasing the impact of local sources. The higher mixing heights in the summer lower background concentrations, but the lower wind speeds also decrease dispersion, increasing the impact of onroad emissions.

The concentrations near roads in HYCAMR are generally high; the values are even higher where major interstate highways merge. In New Haven, we find the highest concentrations where I-95 and I-91 merge and we observe similar behavior in other cities. Compared to NOx, EC concentrations reach background concentrations nearer to the roads. This could result from the relatively lower EC emission rate from onroad sources compared to NOx. We also anticipate that NOx secondary chemistry and interaction with regional pollutant would increase the split between NO and NO_2 allowing greater dispersion of NOx in HYCAMR. Our initial analysis indicates that HYCAMR captures the anticipated qualitative spatial dispersion of primary and secondary species.

HYCAMR estimates yields improved spatial resolution and increased concentration gradients. CAMx estimated NOx concentrations in New Haven ranged from 12.24 ppb to 17.02 ppb in winter, 9.37 ppb to 13.56 ppb in spring, 12.77 ppb to 16.92 ppb in summer, and 10.17 ppb to 15.33 ppb in fall, while HYCAMR estimates ranged from 7.10 ppb to 828 ppb in winter, 5.30 ppb to 520 ppb in spring, 6.25 ppb to 559 ppb in summer, and 5.31 ppb to 618 ppb in fall. Similarly, we find significant differences in the range of EC and $PM_{2.5}$ estimates between CAMx and HYCAMR. This results from the higher resolution of HYCAMR which captures the higher concentration gradients near roads yielding a wider range of predicted concentrations.

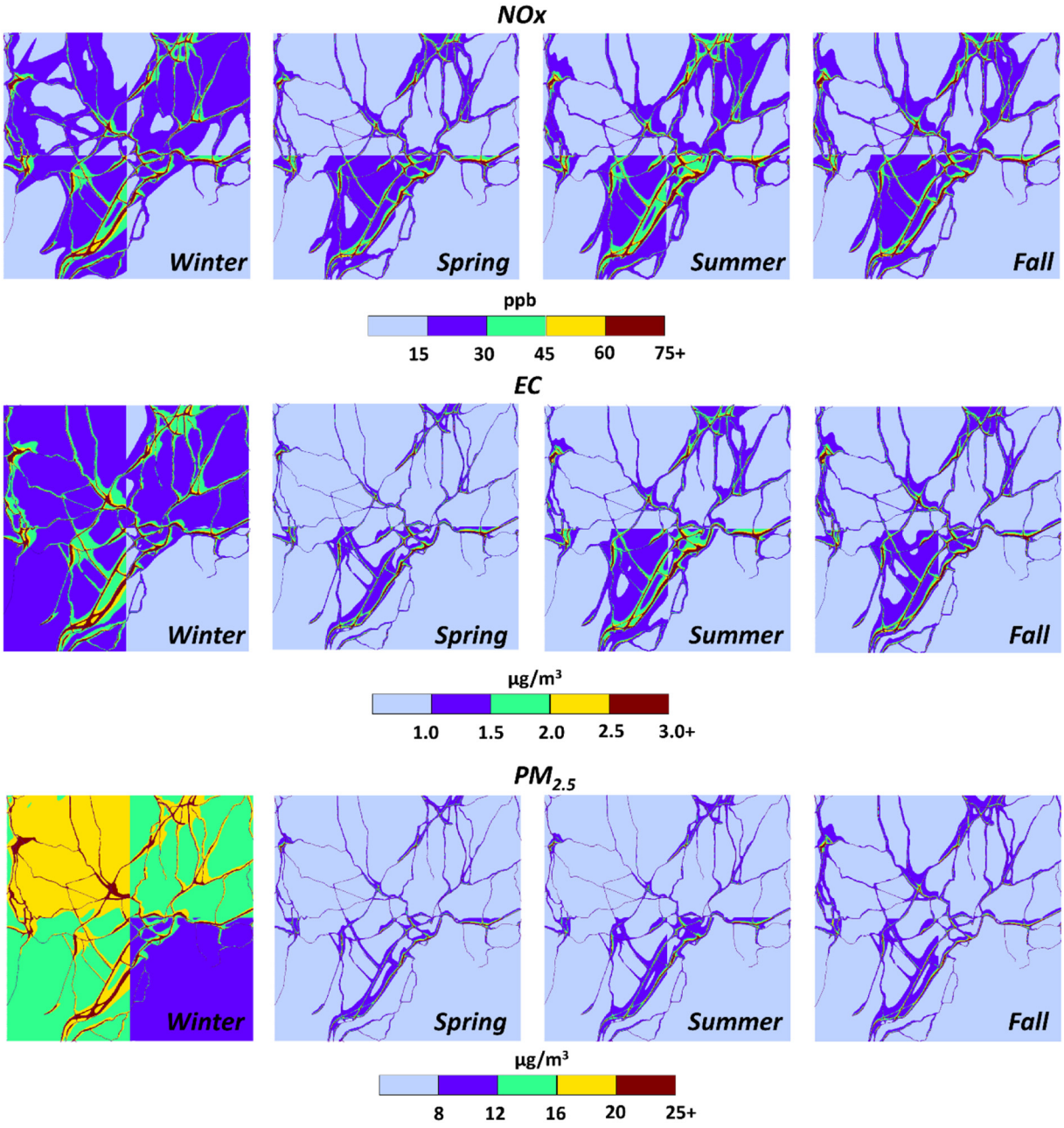

Fig. 2. Average combined concentrations (regional and on-road) of NOx, EC, and $PM_{2.5}$ at 40 m×40 m resolution in winter (December, January, February), spring (March, April, May), summer (June, July, August), and fall (September, October, November) in New Haven, CT.

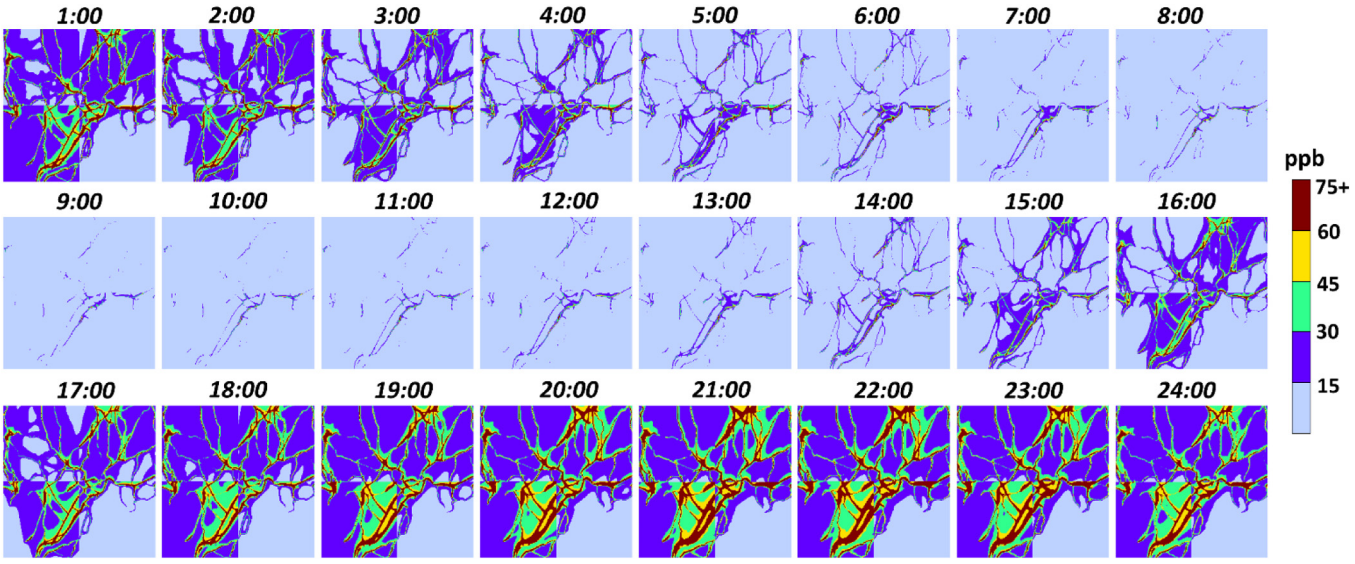

Fig. 3. Annual average hourly NOx concentration in New Haven, CT. We average concentrations over all months of the year 2011 at different hours of each day. We observe significant diurnal variability in NOx concentration.

Between the three locations, the estimated pollutant concentrations in Willimantic are lower than in Hartford and New Haven as Willimantic is a much smaller city and has fewer primary and secondary roads and lower traffic loads (Figs. 2 and S3–S4). Although Hartford does not have as many primary and secondary roads as New Haven it still displays elevated concentrations from vehicular emissions due to the high traffic volume in the city. One of the major benefits of HYCAMR is that it can capture high concentration zones within cities. For instance, we observe heighten concentrations in the urban cores where population densities and traffic loads are highest. We also observe similar high concentration zones near major roads or where multiple major roads intersect.

3.2. Diurnal variation of pollutant concentration

Figs. 3–5 show the annual average hourly concentrations of NOx, EC, and $PM_{2.5}$ for New Haven. We find substantial diurnal variability in concentrations for all three pollutants. Concentrations, especially those near roads, decrease during the day and increase at night. This results from a shift from a dominant unstable atmosphere during the day, which promotes greater mixing, to a dominant stable atmosphere at night. Between the three species, the impact of onroad emissions is less dominate for $PM_{2.5}$, likely because $PM_{2.5}$ results from more regional sources. We see similar trends for Hartford (Figs. S5–S7).

3.3. Near road concentration profiles

Fig. 6 shows the HYCAMR estimated downwind concentration profiles of NOx and EC in New Haven, normalized by the concentrations at the center of the road. We calculate these estimates using several isolated major roads in northern New Haven (State Highway 69, State Highway 63, Amity Rd, and Litchfield Turnpike) to avoid interference with emissions from nearby roads. In order to estimate the decay profile of each pollutant, we first consider the concentration at a specific

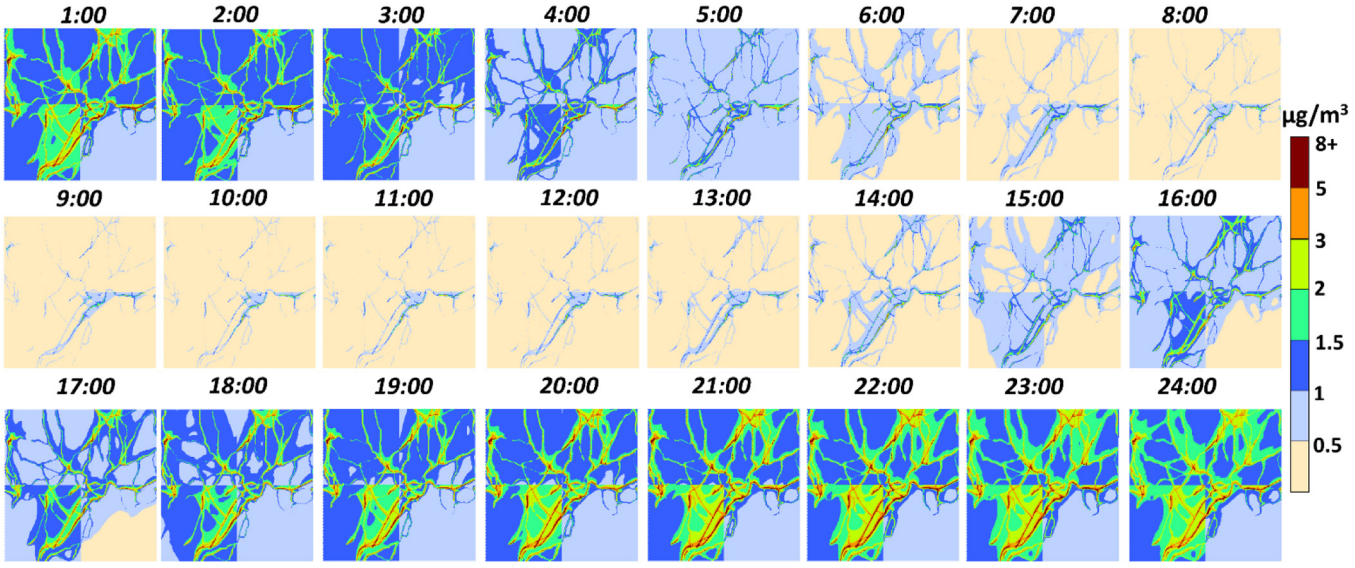

Fig. 4. Annual average hourly elemental carbon (EC) concentration in New Haven, CT. We average concentrations over all months of the year 2011 at different hours of each day. We observe significant diurnal variability in EC concentration.

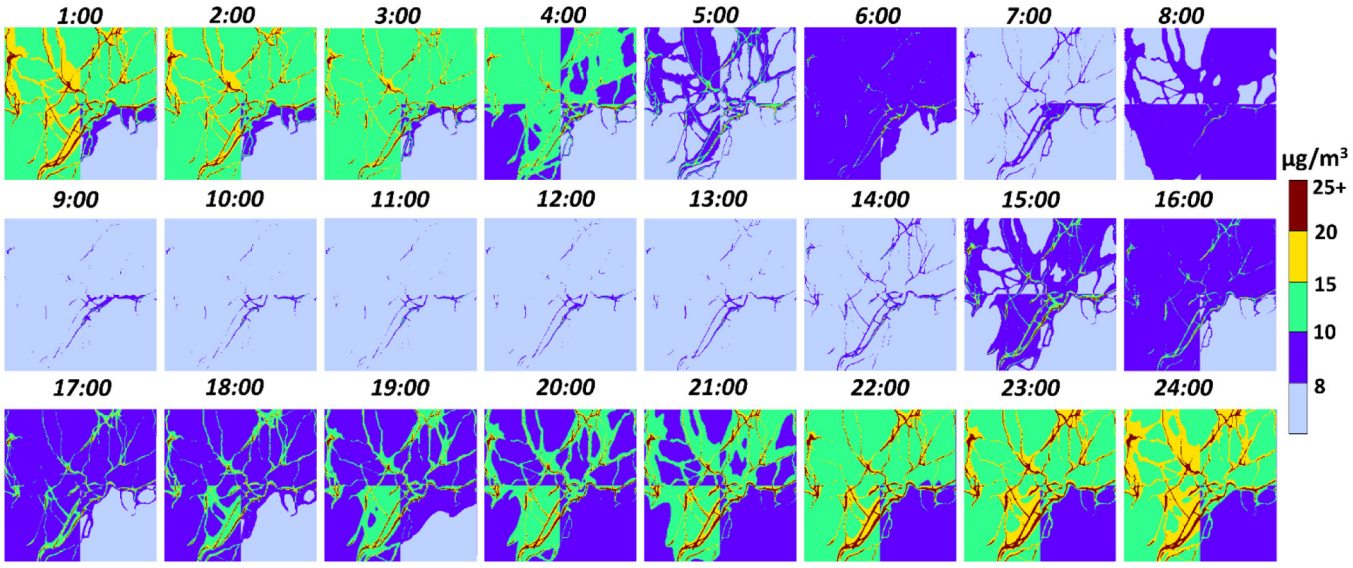

Fig. 5. Annual average hourly $PM_{2.5}$ concentration in New Haven, CT. We average concentrations over all months of the year 2011 at different hours of each day. We observe significant diurnal variability in $PM_{2.5}$ concentration.

downwind distance and then normalize by the concentration at the closest point to the center line of the road. We then average the profiles from multiple roads to create the average profiles shown in Fig. 6. Our results show an exponential decay with distance for all seasons, though the profiles do show substantial differences between seasons and species. As found by Saha et al. (2018), we also find that the differences in decay patterns between species in a single season are less prominent than the differences in decay patterns for the same species in different seasons. Winter shows the slower decay rate anticipated due to dominant stable atmospheric conditions. For instance, in New Haven, NOx concentrations drop by ~40% at 200 m in winter, whereas, in fall and spring, concentrations drop by ~60% over the same distance. These findings are consistent with Beckerman et al. (2008). We observe similar trends for EC. We also find that the higher convective atmosphere and temperature in summer do not impact the decay rate. In fact, we find no significant differences between summer and winter predicted pollutant decay profiles. This indicates that, apart from emissions, wind speed is the major factor influencing dispersion from roads. Lower wind speeds in summer ultimately leads to slow decay rates, while higher wind speeds lead to faster decay rates in fall and spring. Overall, both the species reach background levels within 400 m of the road though EC reaches background levels at shorter distances than NOx. These findings are again consistent with Riley et al. (2014).

3.4. Average exposure concentration

We estimate the average exposure concentration (i.e. the average concentration to which populations are exposed) in each urban area using population-weighted average concentrations. We compare average exposure concentrations at census block group resolution using HYCAMR and CAMx as a first evaluation of the impact of using high resolution modeling for exposure estimation. We use the 2010 census data (US Census Bureau, 2010) to quantify average exposure concentration using Eq. (5).

$$C_{pop,j} = \frac{\sum_i^N C_i \times P_i}{\sum_i^N P_i} \tag{5}$$

In Eq. (5), $C_{pop,j}$ is the average exposure concentration for species j; C_i and P_i are the concentrations and population in census block group i, respectively; and N is the total number of census block groups in a given city. Fig. 7 shows the estimated average exposure concentrations of NOx, elemental carbon (EC), and $PM_{2.5}$ for each season in New Haven and Hartford. Our results show substantial differences in the average exposure concentrations for each season with the highest values in winter. The average exposure concentrations for $PM_{2.5}$ and EC in New Haven

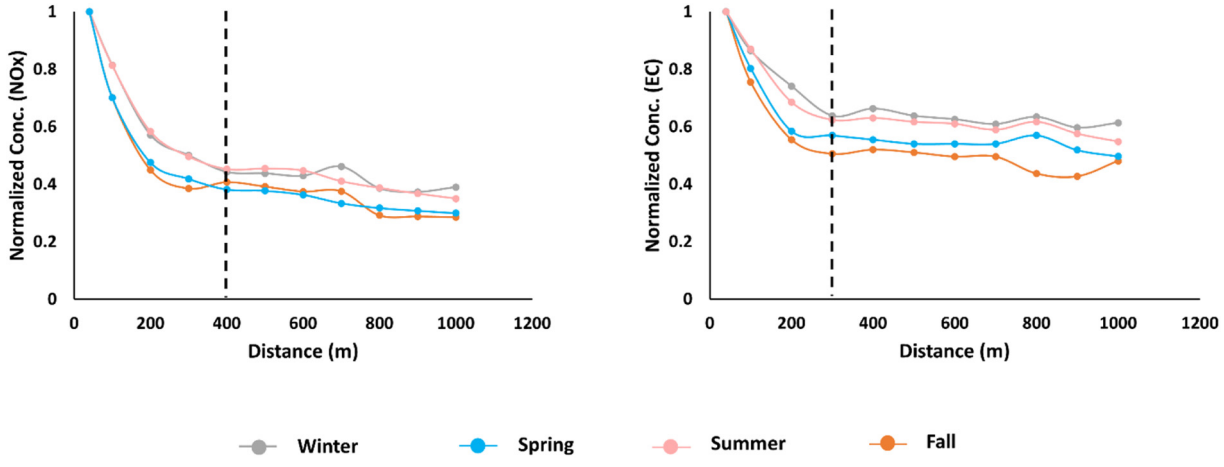

Fig. 6. Downwind concentration decay profiles for NOx and EC in New Haven. The four different lines depict the trend in each season.

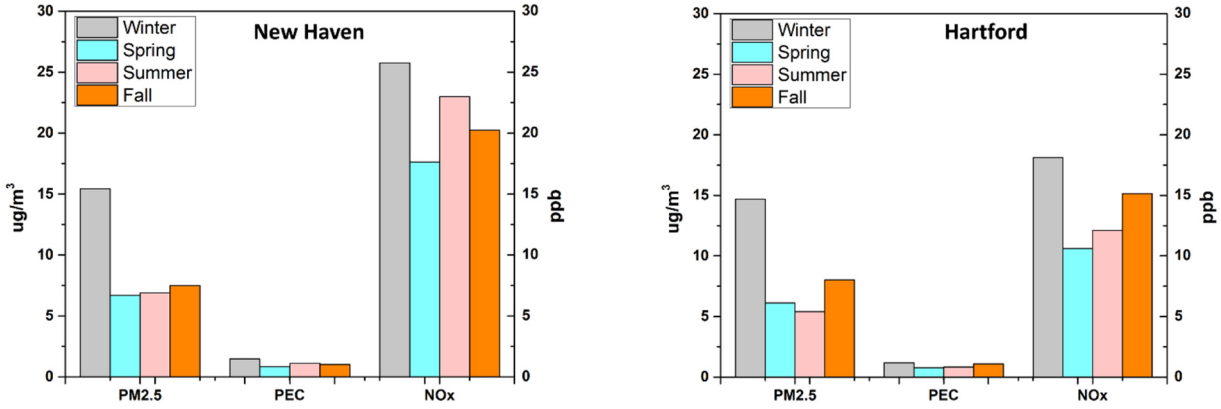

Fig. 7. HYCAMR estimated average exposure concentrations of $PM_{2.5}$, EC, and NOx in New Haven and Hartford in each season. We observe significant seasonal variability.

and Hartford are quite similar; however, the average NOx exposure concentration is significantly higher in New Haven due to the larger number of major roads and denser population in New Haven. When we compare the fine (HYCAMR) and coarse (CAMx) estimates, we find that winter exhibits the largest differences, especially for NOx (Fig. 8). The lower mixing height, slower chemistry, and lower dispersion in winter elevates HYCAMR predicted concentrations near roads leading to these greater differences. The HYCAMR estimated annual average exposure concentrations of NOx are 58% and 13% higher than CAMx for New Haven and Hartford, respectively. This substantial increase in average exposure concentrations using HYCAMR compared to CAMx results from the coarse resolution of regional modeling underestimating the impact of local exposures, particularly as onroad emissions are the major source of NOx. For $PM_{2.5}$, we observe greater differences between fine (HYCAMR) and coarse (CAMx) model estimates. This results because $PM_{2.5}$ is comprised of several species including near road dust and nitrate and the fine resolution of HYCAMR captures the elevated concentrations near roads. This leads to increased differences in average exposure concentrations using HYCAMR compared to CAMx. Unlike our findings for NOx and $PM_{2.5}$, our estimates show that CAMx predicted average exposure EC concentration is slightly higher than HYCAMR. This results from the rapid decay in EC concentrations as distance from the road increases leading to less of the population living in the elevated zone for EC than for $PM_{2.5}$ and NOx.

3.5. Model evaluation

We compare the performance of HYCAMR and CAMx for all three Connecticut cities (New Haven, Hartford, and Willimantic) for NO_2 and $PM_{2.5}$. We present all the statistical parameters summarizing model performance in Tables 1 and S1–S3.

Table 1 shows the comparison between HYCAMR and CAMx over New Haven against both the satellite-based and Kim LUR estimates. For NO_2 satellite-based estimates, the mean fractional bias (MFB) and mean fractional error (MFE) reduce from −1.11 to −0.66 and 1.11 to 0.89, respectively, when comparing CAMx and HYCAMR. This clearly indicates that HYCAMR shows better agreement than CAMx; however, both these model underestimated NO_2 with respect to satellite-based estimates. This could likely results from two factors. First, the approaches use different temporal data when estimating the average NO_2 concentration. Satellite-based estimates use the concentrations at a single time point for each day, whereas HYCAMR and CAMx estimates include concentration estimates for all hours. Second, the datasets provide estimates at different spatial resolution. We also estimate the fraction of HYCAMR and CAMx estimates within a factor of two of reference datasets (FAC2). The FAC2 for NO_2 values are within the limit ($0.5 \leq FAC2 \leq 2$) for HYCAMR, however for CAMx this value is smaller than the expected limit.

We further compare HYCAMR and CAMx estimates to NO_2 concentration estimates from the Kim LUR model at census block group resolution to compare HYCAMR with another high resolution estimate. To compare these estimates, we first up-scale the HYCAMR estimates from 40 m × 40 m resolution to census block group resolution. Both HYCAMR and CAMx show better agreement with Kim LUR estimates than satellite-based estimates. Specifically, the MFB and MFE for NO_2 when compared to Kim LUR estimates are −0.47 and 0.50, respectively, for CAMx and 0.15 and 0.40, respectively, for HYCAMR. This higher agreement likely results from finer resolution (census block group) of the Kim LUR estimates.

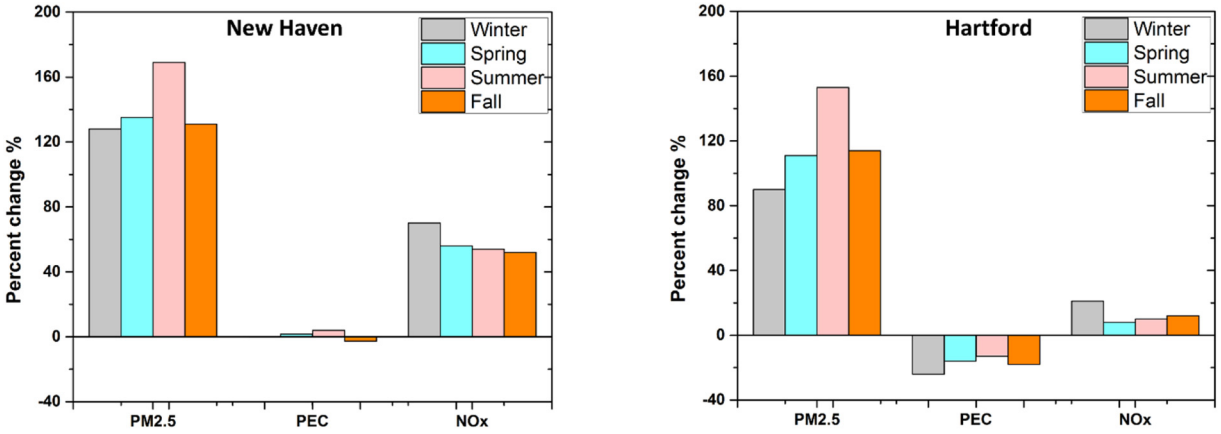

Fig. 8. Percent differences in the estimated average exposure concentrations between HYCAMR and CAMx.

Table 1
Performance evaluation statistics for HYCAMR and CAMx in New Haven using satellite-based and Kim LUR estimations for year 2011.

		MFB	MFE	RMSE	IOA	FAC2	Corr
NO_2	CAMx/Satellite	−1.11	1.11	64.97	0.34	0.30	0.16
	HYCAMR/Satellite	−0.66	0.89	60.78	0.30	0.79	0.13
	CAMx/LUR	−0.47	0.50	7.72	0.24	0.68	−0.22
	HYCAMR/LUR	0.15	0.40	26.44	0.09	1.47	0.20
$PM_{2.5}$	CAMx/GWR	−0.77	0.77	7.45	0.44	0.49	−0.25
	HYCAMR/GWR	−0.11	0.46	5.55	0.29	1.04	−0.26
	CAMx/LUR	−0.85	0.85	5.57	0.11	0.41	0.13
	HYCAMR/LUR	−0.12	0.20	2.22	0.24	0.91	0.22

HYCAMR performs better than CAMx when compared to both estimates of NO_2.

Model performance for $PM_{2.5}$ displays similar trends with HYCAMR showing better agreement than CAMx when compared to both satellite-based and Kim LUR estimates (Tables 1 and S1–S2). However, unlike NO_2, we observe greater differences for $PM_{2.5}$ in HYCAMR and CAMx performance with LUR model data set. This could result from differences in the methods for estimating NO_2 and $PM_{2.5}$ in the reference data sets. We observe similar trends for Hartford and Willimantic (Tables S1–S2).

4. Conclusions

The hybrid air pollutant concentration modeling framework, HYCAMR, described here provides spatially and temporally resolved estimates of pollutant concentrations at high resolution. Implementing this model in three cities in Connecticut, we find strong seasonal and temporal variabilities in pollutant concentrations. Winter shows higher concentrations due to lower mixing heights and turbulence. We also find that concentrations near roads drop during the day due to increased turbulence and instability. Comparing different species, onroad NOx contributes more to the overall concentrations than $PM_{2.5}$ or EC. In alignment with past studies, we find that near road concentrations reach background levels within approximately 400 m of the road. HYCAMR estimated concentrations are also comparable with both satellite-based and land use regression estimates of concentrations. In addition to providing high resolution concentration estimates, HYCAMR has several advantages over many contemporary hybrid models. HYCAMR has relatively low computational and data requirements, captures temporal variability in pollutant concentrations, and applies to a wide suite of species. The two approaches mentioned earlier, Bates et al. (2018) and Chang et al. (2015), either use different methods for gases and particular matter or need individual model runs for each species. These both increase the complexity of model implementation and the required computational time. Compared to these models, HYCAMR not only provides detailed temporal estimates but is also more internally consistent, simpler to implement, and only requires a single run for all species. One of the limitations of the approach is that it does not currently consider unique emissions factors for each road. However, we have demonstrated that HYCAMR is a promising modeling approach in estimating near road pollutant concentrations at high resolution. With the increasing population living and working near roads, high resolution concentration estimates are essential to estimate exposure and eventually develop better policy to mitigate human exposure to air pollution.

Acknowledgment

We would like to acknowledge the Booth Engineering Center for Advanced Technology (BECAT) at the University of Connecticut for the computational resources and technical assistance necessary to carry out this work. This work is supported by the National Science Foundation CAREER Award #1752231 and the Eversource Energy Environmental Engineering Clinic Endowment Fund. We thank Carmen Lamancusa for providing us GEOS-Chem data needed to evaluate model performance.

Appendix A. Supplementary data

Supplementary data to this article can be found online at https://doi.org/10.1016/j.scitotenv.2019.01.218.

References

Adar, S.D., Kaufman, J.D., 2007. Cardiovascular disease and air pollutants: evaluating and improving epidemiological data implicating traffic exposure. Inhal. Toxicol. 19, 135–149. https://doi.org/10.1080/08958370701496012.
Arden Pope, C., Burnett, R.T., Turner, M.C., Cohen, A., Krewski, D., Jerrett, M., Gapstur, S.M., Thun, M.J., 2011. Lung cancer and cardiovascular disease mortality associated with ambient air pollution and cigarette smoke: shape of the exposure-response relationships. Environ. Health Perspect. 119 (11), 1616–1621. https://doi.org/10.1289/ehp.1103639.
Bates, J.T., Pennington, A.F., Zhai, X., Friberg, M.D., Metcalf, F., Darrow, L., Strickland, M., Mulholland, J., Russell, A., 2018. Application and evaluation of two model fusion approaches to obtain ambient air pollutant concentrations at a fine spatial resolution (250 m) in Atlanta. Environ. Model. Softw. 109, 182–190. https://doi.org/10.1016/j.envsoft.2018.06.008.
Batterman, S., Ganguly, R., Harbin, P., 2015. High resolution spatial and temporal mapping of traffic-related air pollutants. Int. J. Environ. Res. Public Health 12 (4), 3646–3666. https://doi.org/10.3390/ijerph120403646.
Beckerman, B., Jerret, M., Brook, J.R., Verma, D.K., Arain, M.A., Finkelstein, M.M., 2008. Correlation of nitrogen dioxide with other traffic pollutants near a major expressway. Atmos. Environ. 42 (2), 275–290. https://doi.org/10.1016/j.atmosenv.2007.09.042.
Beevers, S.D., Kitwiroon, N., Williams, M.L., Carslaw, D.C., 2012. One way coupling of CMAQ and a road source dispersion model for fine scale air pollution predictions. Atmos. Environ. 59, 47–58. https://doi.org/10.1016/j.atmosenv.2012.05.034.
Bell, M.L., Ebisu, K., Belanger, K., 2008. The relationship between air pollution and low birth weight: effects by mother's age, infant sex, co-pollutants, and pre-term births. Environ. Res. Lett. 3 (4), 044003. https://doi.org/10.1088/1748-9326/3/4/044003.
Caiazzo, F., Ashok, A., waitz, I.A., Yim, S.H.L., Barret, S.R.H., 2013. Air pollution and early deaths in the United States. Part I: quantifying the impact of major sectors in 2005. Atmos. Environ. 79, 198–208. https://doi.org/10.1016/j.atmosenv.2013.05.081.
Chang, S.Y., Vizuete, W., Valencia, A., Naess, B., Isakov, V., Palma, T., Breen, M., Arunachalam, S., 2015. A modeling framework for characterizing near-road air pollutant concentration at community scales. Sci. Total Environ. 538, 905–921. https://doi.org/10.1016/j.scitotenv.2015.06.139.
Community Modeling and Analysis System (CMAS), University of North Carolina, 2013. SMOKE v3.6.5 User's Mannual. Retrieved from https://www.cmascenter.org/smoke/documentation/3.6.5/html/ch01s02.html.
Crouse, D.L., Peters, P.A., Van Donkelaar, A., Goldberg, M.S., Villeneuve, P.J., Brion, O., Khan, S., Atari, D.O., Jerret, M., Pope III, C.A., Brauer, M., Brook, J.R., Martin, R.V., Stieb, D., Burnett, R.T., 2012. Risk of nonaccidental and cardiovascular mortality in relation to long-term exposure to low concentrations of fine particulate matter: a Canadian national-level cohort study. Environ. Health Perspect. 120 (5), 708–714. https://doi.org/10.1289/ehp.1104049.
CT, Department of Transportation, 2011. https://www.ct.gov/dot/cwp/view.asp?a=3532&q=330402.
Dedoussi, I.C., Barrett, S.R.H., 2014. Air pollution and early deaths in the United States. Part II: attribution of PM2.5 exposure to emissions species, time, location and sector. Atmos. Environ. 99, 610–617. https://doi.org/10.1016/j.atmosenv.2014.10.033.
Ebisu, K., Bell, M.L., 2012. Airborne $PM_{2.5}$ chemical components and low birth weight in the northeastern and mid-Atlantic regions of the United States. Environ. Health Perspect. (12), 1746–1753 https://doi.org/10.1289/ehp.1104763.
EPA, 2014a. U.S. Regulatory Impact Analysis for the Proposed Revisions to the National Ambient Air Quality Standards for Particulate Matter. U.S. Environ. Prot. Agency (EPA-452/P-14-006).
EPA, 2014b. U.S. Meteorological Model Performance for Annual 2011 Simulation WRF v3.4. U.S. Environ. Prot. Agency, EPA http://www.epa.gov/scram001/.
EPA, U.S., 2015. Support Center for Regulatory Atmospheric Modelling (SCRAM). https://www3.epa.gov/scram001/dispersion_related.htm.
Fann, N., Fulcher, C.M., Baker, K., 2013. The recent and future health burden of air pollution apportioned across U.S. sectors. Environ. Sci. Technol. 47 (8), 3580–3589. https://doi.org/10.1021/es304831q.
Franck, U., Odeh, S., Wiedensohler, A., Wehner, B., Herbarth, O., 2011. The effect of particle size on cardiovascular disorders - the smaller the worse. Sci. Total Environ. 409 (20), 4217–4221. https://doi.org/10.1016/j.scitotenv.2011.05.049.
GEOS-Chem V9-02 benchmark history, 2017. http://wiki.seas.harvard.edu/geos-chem/index.php/GEOS-Chem_v9-02_benchmark_history.
Greco, S.L., Wilson, A.M., Spengler, J.D., Levy, J.I., 2007. Spatial patterns of mobile source particulate matter emissions-to-exposure relationships across the United States. Atmos. Environ. 41 (5), 1011–1025. https://doi.org/10.1016/j.atmosenv.2006.09.025.
HEI, 2010. In: Health Effects Institute (Ed.), Traffic-related Air Pollution: a Critical Review of the Literature on Emissions, Exposure, and Health Effects, pp. 1–386 (Special Re (January)).
Isakov, V., Irwin, J.S., Ching, J., 2007. Using CMAQ for exposure modeling and characterizing the subgrid variability exposure estimates. J. Appl. Meteorol. Climatol. 46 (9), 1354–1371. https://doi.org/10.1175/JAM2538.1.

Jerrett, M., Shankardass, K., Berhane, K., Gauderman, W.J., Kunzli, N., Avol, E., Gilliland, F., Lurmann, F., Molitor, J.N., Molitor, J.T., Thomas, D.C., Peters, J., McConnell, R., 2008. Traffic-related air pollution and asthma onset in children: a prospective cohort study with individual exposure measurement. Environ. Health Perspect. 116 (10), 1433–1438. https://doi.org/10.1289/ehp.10968.

Kim, K.-H., Kabir, E., Kabir, S., 2015. A review on the human health impact of airborne particulate matter. Environ. Int. 74, 136–143. https://doi.org/10.1016/j.envint.2014.10.005.

Kim, S.-Y., Bechle, M., Hankey, S., Sheppard, L., Szpiro, A.A., Marshall, J.D., 2018. A Parsimonious Approach for Estimating Individual-level Concentrations of Criteria Pollutants Over the Contiguous U.S (In Preparation).

Lamsal, L.N., Martin, R.V., Van Donkelaar, A., Steinbacher, M., Celarier, E.A., Bucsela, E., Dunlea, E.J., Pinto, J.P., 2008. Ground-level nitrogen dioxide concentrations inferred from the satellite-borne Ozone Monitoring Instrument. J. Geophys. Res. Atmos. 113 (16), 1–15. https://doi.org/10.1029/2007JD009235.

Laughner, J.L., Zare, A., Cohen, R.C., 2016. Effects of daily meteorology on the interpretation of space-based remote sensing of NO_2. Atmos. Chem. Phys. 16 (23), 15247–15264. https://doi.org/10.5194/acp-16-15247-2016.

Loomis, D., Grosse, Y., Lauby-Secretan, B., Ghissassi, F., Bouvard, V., Benbrahim-Talla, L., Guha, N., Baan, R., Mattock, H., Straif, K., 2013. The carcinogenicity of outdoor air pollution. Lancet Oncol. 14 (13), 1262–1263. https://doi.org/10.1016/S1470-2045(13)70487-X.

Parvez, F., Wagstrom, K., 2018. Comparing estimates from the R-LINE near road dispersion model using model-derived and observation-derived meteorology. Atmos. Pollut. Res. 9 (3), 483–493. https://doi.org/10.1016/j.apr.2017.10.007.

Parvez, F., Lamancusa, C., Wagstrom, K., 2017. Primary and secondary particulate matter intake fraction from different height emission sources. Atmos. Environ. 165, 1–11. https://doi.org/10.1016/j.atmosenv.2017.06.011.

Pascal, M., Falq, G., Wagner, V., Chatignoux, E., Corso, M., Blanchard, M., Host, S., Pascal, L., Larrieu, S., 2014. Short-term impacts of particulate matter (PM10, PM10–2.5, PM2.5) on mortality in nine French cities. Atmos. Environ. 95, 175–184. https://doi.org/10.1016/j.atmosenv.2014.06.030.

Pope, C.A., Ezzati, M., Dockery, D.W., 2009. Fine-particulate air pollution and life expectancy in the United States. N. Engl. J. Med. 360 (4), 376–386. https://doi.org/10.1056/NEJMsa0805646.

Riley, E.A., Banks, L., Fintzi, J., Gould, T.R., Hartin, K., Schaal, L., Davey, M., Sheppard, L., Larson, T., Yost, M.G., Simpson, C.D., 2014. Multi-pollutant mobile platform measurements of air pollutants adjacent to a major roadway. Atmos. Environ. 98, 492–499. https://doi.org/10.1016/j.atmosenv.2014.09.018.

Rohr, A.C., Habre, R., Godbold, J., Moshier, E., Schachter, N., Kattan, M., Grunin, A., Nath, A., Coull, B., Koutrakis, P., 2014. Asthma exacerbation is associated with particulate matter source factors in children in New York City. Air Qual. Atmos. Health 7 (2), 239–250. https://doi.org/10.1007/s11869-013-0230-y.

Saha, P.K., Khlystov, A., Snyder, M.G., Grieshop, A.P., 2018. Characterization of air pollutant concentrations, fleet emission factors, and dispersion near a North Carolina interstate freeway across two seasons. Atmos. Environ. 177 (April 2017), 143–153. https://doi.org/10.1016/j.atmosenv.2018.01.019.

Salam, M.T., Islam, T., Gilliland, F.D., 2008. Recent evidence for adverse effects of residential proximity to traffic sources on asthma proximity. Curr. Opin. Pulm. Med. 14, 3–8. https://doi.org/10.1097/MCP.0b013e3282f1987a.

Schwartz, J., Coull, B., Laden, F., Ryan, L., 2008. The effect of dose and timing of dose on the association between airborne particles and survival. Environ. Health Perspect. 116 (1), 64–69. https://doi.org/10.1289/ehp.9955.

Skamarock, W.C., Klemp, J.B., Dudhia, J., Gill, D.O., Barker, D.M., Duda, M.G., Huang, X., Wang, W., Powers, J.G., 2008. A description of the advanced research WRF Version 3. Tech. Rep. (June), 113 https://doi.org/10.5065/D6DZ069T.

Snyder, M.G., Venkatram, A., Heist, D.K., Perry, S.G., Petersen, W.B., Isakov, V., 2013. RLINE: a line source dispersion model for near-surface releases. Atmos. Environ. 77, 748–756. https://doi.org/10.1016/j.atmosenv.2013.05.074.

Turner, M.C., Krewski, D., Pope III, C.A., Chen, Y., Gapstur, S.M., Thun, M.J., 2011. Long-term ambient fine particulate matter air pollution and lung cancer in a large cohort of never-smokers. Am. J. Respir. Crit. Care Med. 184 (12), 1374–1381. https://doi.org/10.1164/rccm.201106-1011OC.

United States Census Bureau, 2010. http://www.census.gov/topics/population/data.html.

United States Department of Agriculture, 2015. https://gdg.sc.egov.usda.gov/GDGOrder.aspx.

Van Donkelaar, A., Martin, R.V., Brauer, M., Hsu, N.C., Kahn, R.A., Levy, R.C., Lyapustin, A., Sayer, A.M., Winker, D.M., 2016. Global estimates of fine particulate matter using a combined geophysical-statistical method with information from satellites, models, and monitors. Environ. Sci. Technol. 50 (7), 3762–3772. https://doi.org/10.1021/acs.est.5b05833.

Vette, A., Burke, J., Norris, G., Landis, M., Batterman, S., Breen, M., Isakov, V., Lewis, T., Gilmour, M.I., Kamal, A., Hammod, D., Vedantham, R., Bereznicki, S., Tian, N., Croghan, C., Community Action Against Asthma Steering Committee, 2013. Sci. Total Environ. 448, 38–47. https://doi.org/10.1016/j.scitotenv.2012.10.072.

Wilhelm, M., Ghosh, J.K., Su, J., Cockburn, M., Jerret, M., Ritz, B., 2012. Traffic-related air toxics and term low birth weight in Los Angeles County, California. Environ. Health Perspect. 120 (1), 132–138. https://doi.org/10.1289/ehp.1103408.

Winquist, A., Schauer, J.J., Turner, J.R., Klein, M., Sarnat, S.E., 2015. Impact of ambient fine particulate matter carbon measurement methods on observed associations with acute cardiorespiratory morbidity. J. Expo. Sci. Environ. Epidemiol. 25 (2), 215–221. https://doi.org/10.1038/jes.2014.55.

Yarwood, G., Jung, J., Whitten, G.Z., Heo, G., Melberg, J., Estes, M., 2010. Updates to the carbon bond mechanism for version 6 (CB6). Presented at the 9th Annual CMAS Conference, Chapel Hill, NC, October 11–13. 6(415), pp. 1–4.